TASK QUARTERLY 6 No 1 (2002), 39–61

TURBOMACHINERY COMPONENT DESIGN BY MEANS OF CFD

RENE A. VAN DEN BRAEMBUSSCHE

Turbomachinery and Propulsion Department – von Karman Institute, Waterloose steenweg 72, B-1640 Sint-Genesius-Rode, Belgium
vdb@vki.ac.be

(Received 10 July 2001)

Abstract: A short overview of the main techniques for turbomachinery blade design based on CFD is followed by a more detailed description on an Optimisation- and Inverse Design method, developed at the von Karman Institute. The optimisation method uses an Artificial Neural Network to extract knowledge from a Database containing the results of previous designs and a Genetic Algorithm to define the optimum blade. The inverse design method makes use of the Euler or Navier-Stokes equations to predict how a given 3D blade shape should be modified to reach a prescribed pressure or Mach number distribution along the blade surface. Examples of transonic compressor and turbine blades, designed by both methods, illustrate the potential of these modern aero-design systems. Special attention is given to the problems related to existence and uniqueness and to those features that facilitate the practical use of these methods.

Keywords: turbomachinery, blade design, optimisation, inverse design

1. Introduction

CFD has seen a very important development over the last 25 years and has reached a high level of reliability. Navier-Stokes solvers are now routinely used to study fluid flows, in the same way Finite Element Analysis is used for stress predictions. They provide detailed information about the flow around existing blade shapes in a relatively short time and as such constitute an attractive alternative for detailed flow measurements. Complex flow phenomena are now studied in what is called "Numerical Laboratories". This approach is especially attractive for geometries that are difficult to study experimentally, such as flows in rotating components, or even impossible, such as flows in MEMS. Although this has resulted in a drastic decrease of the number of prototype testing, there are still two problems that prevent a more efficient use of CFD in the design process.

The first one results from the difficulty to present a 3D flow on a 2D screen or drawing. Vector plots in a 2D cross section are only a poor presentation of the reality. They can be very misleading as they may suggest that the flow is penetrating the solid walls and 2D projections of streamlines do not always seem to satisfy continuity (Figure 1). Synthetic environments, also called virtual reality, are very promising in

this respect. These techniques will not remain restricted to computer games but will become part of the everyday reality for engineers in the next decade [1]. Designers will walk inside blade rows and diffusers to inspect the complex 3D flow structures by following 3D streamlines and to verify the effect of geometrical changes.

The second problem relates to the abundance of information provided by the Navier-Stokes calculations. Three velocity components, pressure and temperature in typically 10 000 points (2D flow) or in up to 1 000 000 points (3D flow) is more than what the human brain is able to grasp and fully exploit in new designs. Navier-Stokes solvers do not provide information on how to modify the geometry to improve the performance. One needs new tools to use this information in a more efficient way than with the traditional trial and error procedure in which the systematic testing of blade shapes has been replaced by Navier-Stokes calculations. Such iterative design procedures are very time consuming and the outcome depends to a large extent on the experience of the designer.

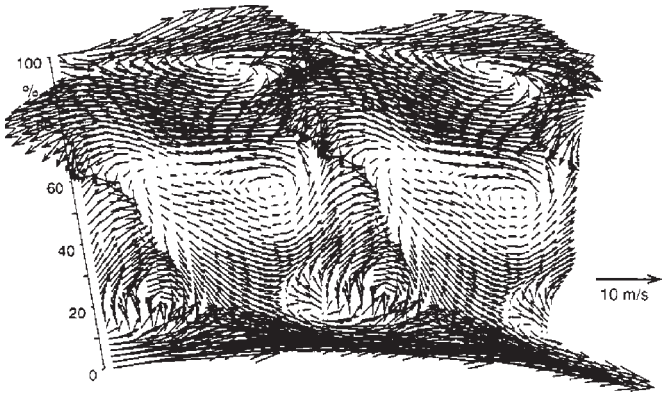

Figure 1. 2D view of the 3D flow at the exit of a turbine stage

This can be problematic in the present context where experienced designers are replaced by young engineers, who may be highly skilled computer and CFD experts but may have limited knowledge about turbomachinery flows. Designers can hardly be expert in all disciplines that interfere with a design (aerodynamics, mechanics, manufacturing *etc.*). Special techniques to support the designers are therefore very desirable.

Modern CFD tools solve the flow equations for prescribed boundary conditions on the borders of the numerical domain. As these borders are the outcome of the design problem, the design procedure needs to be iterative. Different design methods differ by the way the design targets are defined and the procedures to define the required modifications of the geometry.

In what follows one will get a short overview of optimisation and inverse design methods with application to turbomachinery blade design. More details will be provided about the methods that have been developed at the von Karman Institute during the last decade and on some of the special features that make them more easily applicable in a real design environment.

2. Optimisation

Optimisation systems search for the geometry $X(m)$ $m=1,m_{\max}$ corresponding to a minimum value of an Objective Function (OF) while satisfying the Boundary Conditions (BC), mechanical constraints and flow equations $R(X,U)=0$.

In order to reduce the number of unknowns ($m_{\max}$) most optimisation processes make use of a parameterised definition of the geometries based on Bézier curves. This also assures smoothness of the blade surfaces and facilitates the transfer of data to CAD-CAM systems. It is however important that the geometry definition allows a very wide variety of blade shapes without excluding any physically acceptable geometry (Figure 2). Pierret [2] has shown that between 15 and 20 parameters are required.

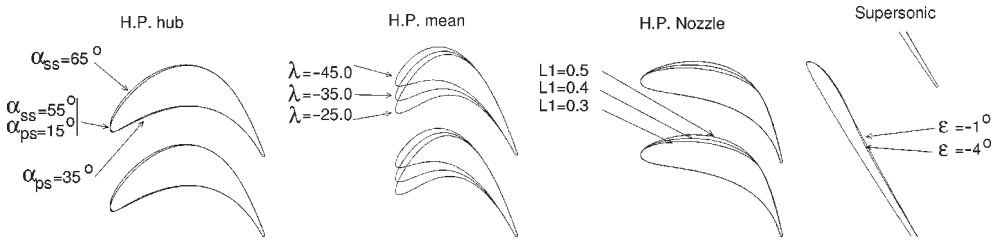

Figure 2. Typical turbine blade geometries

A comprehensive overview of classical optimisation techniques for engineering problems is given by Vanderplaats [3]. Gradient methods are commonly used in many engineering applications to find the optimum combination of geometrical parameters. The basic idea is illustrated in Figure 3 for a simplified problem ($m_{\max}=2$). Starting form an initial geometry (x_1^o,x_2^o) one progressively approaches the optimum combination of x_1 and x_2, corresponding to the minimum value of the OF by marching in the direction S corresponding to the maximum value of $\frac{d(OF)}{ds}$. Each step requires $m_{\max}+1$ Navier-Stokes calculations to find the direction of the maximum gradient and at least one calculation to define the optimum step length. Steps are limited by the constraints, shown by dashed lines in Figure 3. Assuming that n steps are needed, one optimisation will require $n*(m_{\max}+2)$ Navier-Stokes calculations, so that about 340 Navier-Stokes solutions will be needed to perform 20 optimisation steps on a real application with a 15 parameter geometry.

A drastic reduction in the computational effort can be obtained by using the adjoint equations method to calculate the gradients. This mathematically rather complex method is of interest only in combination with implicit solvers. It still requires a full solution at each optimisation step and at least a similar amount of computational effort, using the transpose of the Jacobian of the implicit solver, to calculate the gradient. It is also not easy to formulate a target in function of the local flow variables.

An alternative approach is a systematic sweep of the design space by calculating the OF for different values of x_1 and x_2. Defining only 3 values for each variable between the maximum and minimum limits, means that $3^{m_{\max}}$ Navier-Stokes calculations will be required. This is a valid alternative for problems with a small value of $m_{\max}$ but requires more than $14\cdot10^6$ calculations for $m_{\max}=15$.

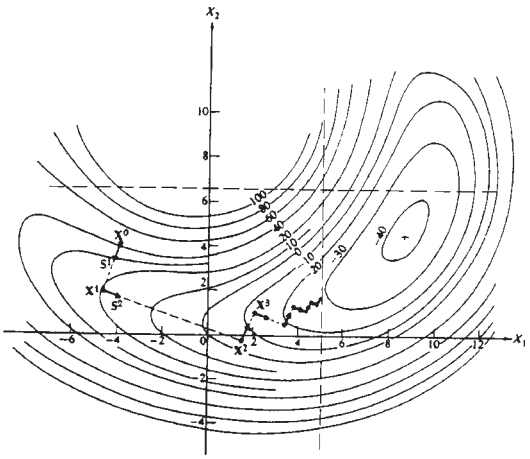

Figure 3. Steepest gradient method

2.1. Optimisation by Evolutionary theory

Evolutionary strategies such as Genetic Algorithms and Simulated Annealing allow a drastic acceleration of the procedure by replacing the systematic sweep by a more intelligent selection of new geometries using information obtained during previous designs. Such a procedure applied to a turbine blading is schematically shown in Figure 4.

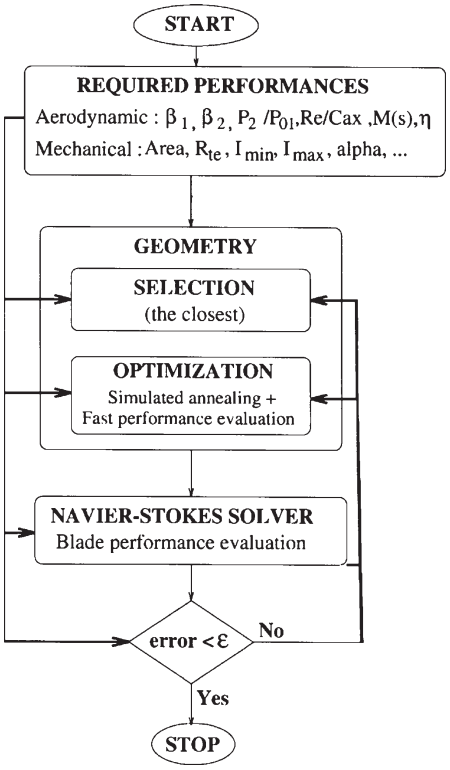

Figure 4. Simple GA optimisation system

The design of a new blade starts from the definition of the REQUIRED PERFORMANCES. In the case of a 2D turbine blade it consists of: aerodynamic requirements (inlet and outlet flow angles β_1, β_2, the pressure ratio P_2/P_1^0, Reynolds number over axial chord ratio $\mathrm{Re}/C_{\mathrm{ax}}$) and mechanical constraints *i.e.* blade cross-section area (Area), trailing edge radius (R_{TE}), minimum and maximum moment of inertia ($I_{\min}$ and $I_{\max}$), and the angle α (alpha) between $I_{\max}$ and the axial direction. This is where the aero design is linked to a mechanical blade analysis and to a preliminary optimisation of the complete turbine layout by means of a 1D or 2D through-flow analysis method. These requirements have a different formulation for axial and radial compressors.

Starting from an initial blade geometry, defined by Bézier curves as a function of 15 parameters $X(15)$, a first generation of blades is created by randomly perturbing the 15 parameters. Each of them is analysed by the Navier-Stokes solver and the OF is calculated. The different geometries and their corresponding OF are then used to guide the Genetic Algorithm in defining the next generation of blades, which are supposed to be closer to the optimum. The Genetic Algorithm simulates the selection process that takes place in nature by which the fittest species (low OF) have more chances to survive than the weaker ones (high OF). Although the number of required calculations can be drastically reduced by this technique the optimisation is still very time consuming because each specimen must be analysed with the very costly Navier-Stokes solver.

A drastic reduction in computational effort can be achieved by making a first optimisation by means of a rapid evaluation system and only the final check with a more reliable Navier-Stokes solver. It is however important that the fast evaluation gives results that are consistent with the full 3D solver to avoid that the optimisation is driven in a wrong direction. The method developed at the von Karman Institute [2, 4–7] uses a fast performance evaluation model based on an Artificial Neural Network and the results of previous designs and analyses contained in the DATABASE (Figure 5). The ANN takes only a fraction of the time needed by a Navier-Stokes calculation so that a large number of geometries can be evaluated in a very short time. The geometry, once optimised by means of this fast but approximate flow analyser, is then verified by the more accurate but also much more expensive Navier-Stokes solver. The procedure stops when the Navier-Stokes solver predicts that the target is reached. Otherwise the "not yet optimum" geometry and the corresponding result of the Navier-Stokes calculation are added to the DATABASE and a new learning of the ANN is started. It is expected that the ANN becomes more accurate at each iteration as the learning will make use of new information about geometries that are close to what is desired. The whole loop is repeated until the Navier-Stokes solver confirms that the geometry is optimal.

The results stored in the DATABASE are: the aerodynamic requirements, geometrical parameters, efficiency and Mach number distribution obtained form the Navier-Stokes solver.

An Artificial Neural Network (ANN) (Figure 6) is used to construct the fast performance evaluation model by approximating the Navier-Stokes solver based on the information contained in the DATABASE. It is composed of several elementary

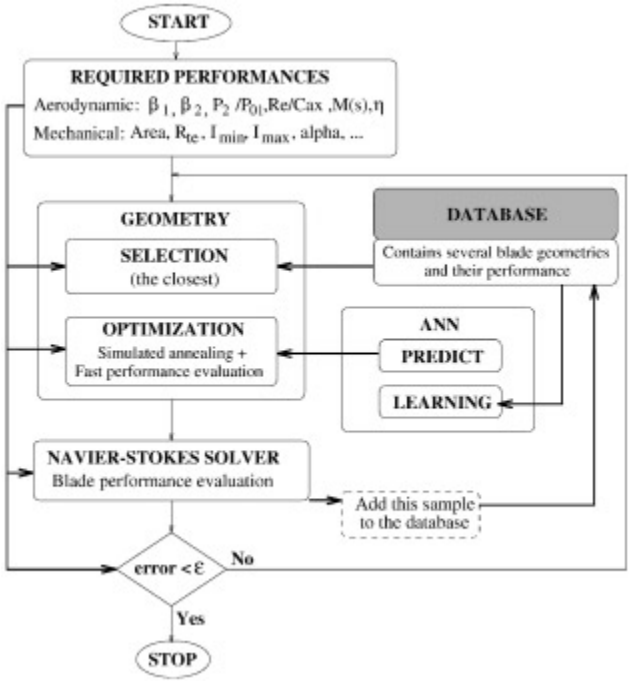

Figure 5. General algorithm of the GA and ANN design method

processing units called neurons or nodes. These nodes are organised in layers and joined with connections (synapses) of different intensity, called the connection weight (W) to form a parallel architecture. Each node performs two operations: the first one is the summation of all the incoming signals and the second one is the transformation of the signal by using a transfer function, very often defined by a sigmoidal function: $FT(x) = \frac{1}{1+e^{-x}}$. This function introduces power series (given implicitly in the form of an exponential term) and does not require any hypotheses concerning the type of relationship between the input and the output variables. A network is generally composed of several layers; an input layer, zero, one or more hidden layers and one output layer. The coefficients are defined by a LEARNING procedure relating performance P_i (*i.e.* η, β_2 and the Mach number distribution $M(I) I = 1{,}40$) to the boundary conditions BC_i and geometry G_i.

After training the ANN on an available representative set of input and output vectors by the LEARNING process, it is able to generalise, meaning that it can PREDICT the performance of a new geometry which is not present in the DATABASE.

Figure 7 compares the Mach number distribution predicted by the Navier-Stokes solver with the one obtained from the neural network trained with a database containing 25 samples. The agreement is surprisingly good. As the time for LEARNING is proportional to the number of training samples, it is sometimes of interest to build a sub-database (training database) containing only blade samples that are similar to the blade being designed.

The computational time needed for the training of an ANN and to run the optimisation algorithm are respectively 10% and 25% of the time needed by the Navier-Stokes solver. A complete design cycle including blade design, optimisation

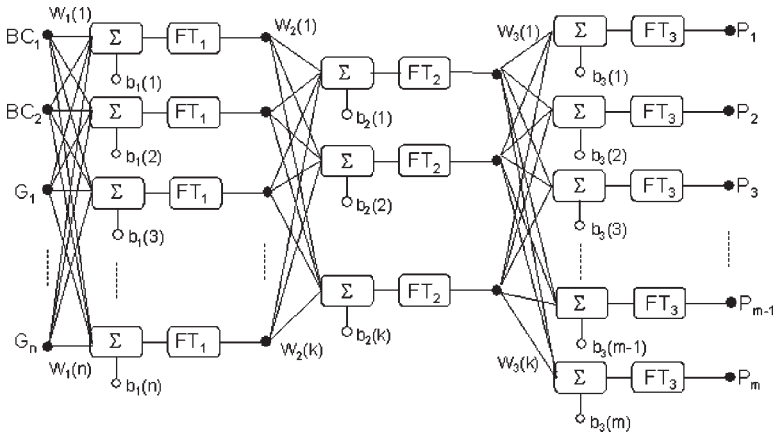

Figure 6. A 3-layer Artificial Neural Network

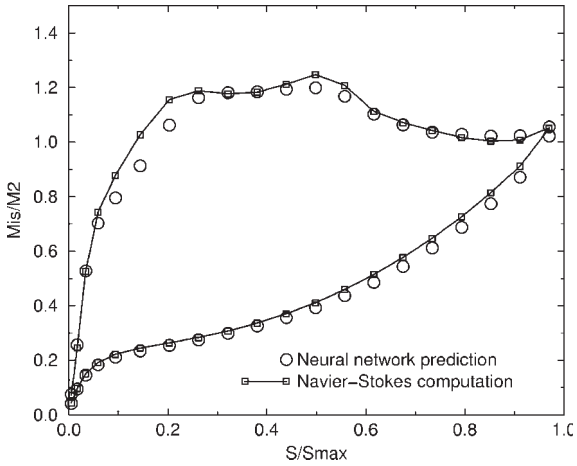

Figure 7. Mach number distribution predicted by ANN and Navier-Stokes solver

and verification by means of a Navier-Stokes solver needs only 35% more time than one single Navier-Stokes analysis. The main computational effort is the construction of a new database when starting a new application.

The global performance, measuring the quality of flow and respect of the aerodynamic and mechanical constraints, is used at several steps in the design procedure, *i.e.* during the optimisation process and for the convergence check after the Navier-Stokes calculation. The general approach to this problem is to build a single objective function (OF) which is the summation of penalty terms that increase when the constraints are violated.

Following is an example of a global objective function:

$$OF = P_{\text{Meca}} + P_{\text{Perf}} + P_{\text{Geom}} + P_{\xi} + P_{\text{Mach}} + P_{\text{manuf}} + \ldots$$

where:

P_{Meca} is the penalty that increases when violating the mechanical constraints. In a first approach it can be based on simple correlations and past experience.

Similar to what is done for the aero-performance it should be verified in a later step by a more accurate technique.

P_{Perf} is the penalty for not achieving the required aerodynamic performance (outlet flow angle, mass flow,...).

P_{Geom} is the penalty for violating geometrical constraints. These constraints may take into account manufacturing and assembly techniques, weight, *etc.* ... External modules may be needed to calculate the value.

P_ξ is the penalty for non optimum performance. It is directly proportional to the loss coefficient.

P_{Mach} stands for the penalty for non-optimum Mach number distribution. This penalty has been introduced in addition to the one based on the loss coefficient because:

- the loss coefficient predicted by a Navier-Stokes solver is not sufficiently reliable to be used as the only criterion. Uncertainties in the turbulence and transition modelling can result in discontinuous variations of P_ξ.
- losses may have multiple local minima or can show large gradients when the transition point suddenly jumps from a near leading edge to near trailing edge position.
- blades need to perform well also at off-design conditions and controlling the Mach number distribution, one can account for the changes that are likely to occur at off-design.

The penalty function on the Mach number distribution is based on a simplified calculation of the pressure and suction side boundary layer and an estimation of transition in function of pressure gradient and free stream turbulence. The purpose is to give high penalty to velocity distributions that are known of not being optimal such as distributions with a high probability of early transition, laminar or turbulent separation. It replaces the visual inspection of the Mach number distribution by an experienced designer. A more detailed description is given in [5].

The above Objective Function is only an example. The user can easily extend it to include other design criteria, such as manufacturing cost (P_{manuf}), maintainability or by changing the relative weight of each term.

2.2. 2D turbine blade design

Previous design procedure has been successfully tested on a large number of designs and will be illustrated here by the design of a transonic reaction-type blade. The imposed parameters together with the mechanical and aerodynamic requirements are summarised in Table 1 in which also the requirements are compared with the values obtained after 18 design cycles *i.e.* 18 Navier-Stokes Calculations.

This design was started from a DATABASE containing 25 samples and the sample with the lowest OF has been used as starting geometry. The Mach number distribution on the initial geometry has a shock at mid-chord on the suction side (Figure 8). The low velocity on the pressure side and the little peak on the suction side near the leading edge indicate a too large incidence for this blade. After a first design iteration the incidence is already reduced by changing the stagger angle

Table 1. Imposed parameters, mechanical and aerodynamic requirements

β_1 flow(o)	18.0
M_2^{is}	0.9
Re	5.8 10.5
γ=Cp/Cv	1.4
Tu(%)	4
$C_{ax}(m)$	0.052
Pitch/C_{ax}	1.0393
TE thick (m)	1.2 10.-3

	Imposed		After
	Min.	Max.	18 modif.
surface	5.2 10.-4	6.8 10.-4	5.36 10.-4
$I_{min}(m4)$	7.5 10.-9	1.2 10.-8	7.45 10.-9
$I_{max}(m4)$	1.25 10.-7	2.2 10.-7	1.28 10.-7
α_{Imax}	-50.00	-30.00	-37.50
β_2 flow(o)	-57.80	57.80	-57.62
loss coef.(%)	0.0	0.0	1.9

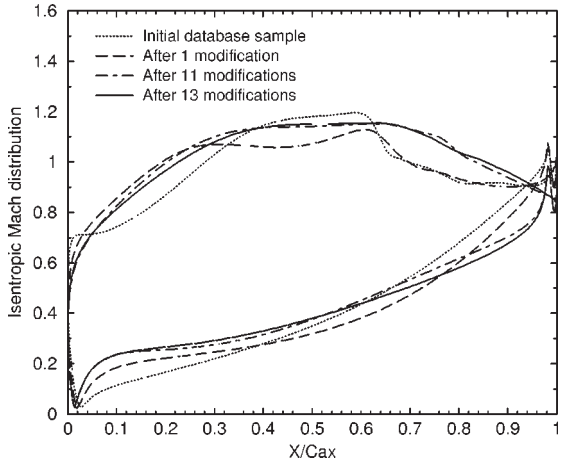

Figure 8. Evolution of the Mach number distribution with design iteration

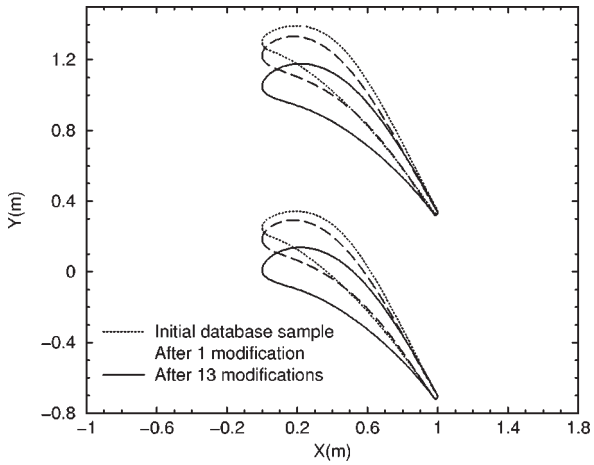

Figure 9. Variation of blade geometries

(Figure 9). Also the shock strength is decreased and has completely disappeared after 13 iterations.

The discrepancy between the objective function, predicted by the ANN, and the one based on the Navier-Stokes solution at different design cycles is shown in Figure 10. The ANN predicts a rapid decrease of the penalty function during the

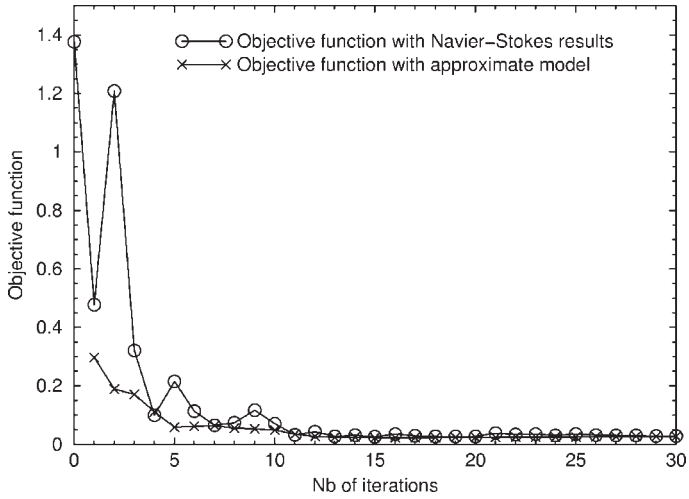

Figure 10. Design convergence history

first 5 design cycles, whereas the Navier-Stokes shows large oscillations up to the 10^{th} iteration.

This discrepancy is due to an imperfect prediction by the ANN driving the GA towards an optimum which, according to the Navier-Stokes solver, is not as good as predicted. The inaccuracy of the fast prediction method is a consequence of the incomplete information contained in the DATABASE. However by adding each time the new geometry and corresponding solution to the DATABASE one gradually completes the knowledge and the ANN becomes more accurate at each design loop. The final result is a turbine blade with shock free transonic flow and a loss coefficient as low as 1.9%. It is obtained by a fully automated procedure after 13 Navier-Stokes calculations. The additional iterations do not really improve the result and have been made to verify that the agreement between both predictions was not accidental.

2.3. 3D blade design

The second example illustrates the extension of the method to Q3D blade design. This procedure (Figure 11) starts by defining a series of N 2D blade sections, using the 2D design procedure and stacking them along a prescribed lean and sweep line. The resulting 3D geometry is then analysed by means of a 3D Navier-Stokes solver to verify that the 3D requirements are satisfied. Eventual discrepancies are used to adjust the 2D requirements after which the procedure is repeated. An alternative approach could be to calculate the penalties from the results of the 3D analysis.

An important part of the losses in a multistage machine is due to the spanwise non-uniformity of the inlet flow angle, resulting from the non-uniformity of the outlet flow of the preceding blade row. The present design therefore aims for the linear variation of the outlet flow angle indicated by circles in Figure 12 in five equidistant radial positions between hub and tip.

After the first iteration, the predicted outlet flow angle, represented by the dashed line, is far from the required one (the circles), especially at the tip. The outlet flow angle imposed for the 2D design is modified accordingly (the triangles) to counteract the outlet angle changes due to 3D flow effects. After the third design

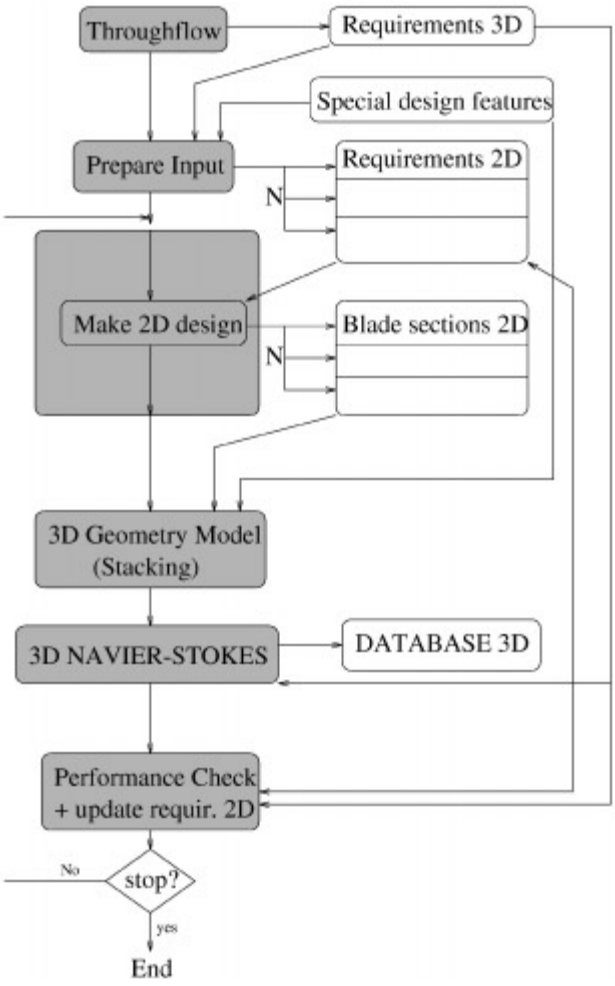

Figure 11. Flow chart of the three-dimensional design procedure

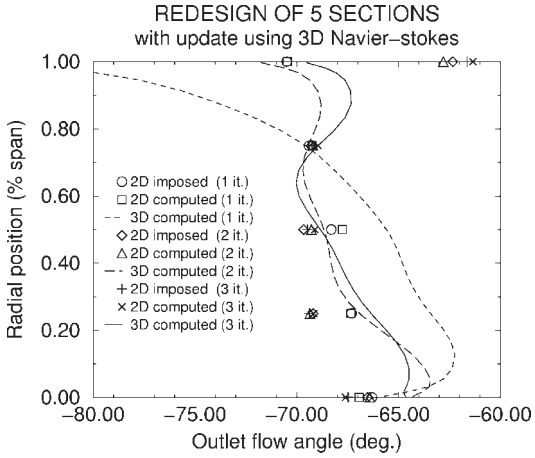

Figure 12. Spanwise variation of the blade to blade outlet flow angle

iteration, the outlet flow angle, obtained with the 3D Navier-Stokes solver (the solid line in Figure 12) is much closer to the target one. A further improvement of the uniformity of the outlet flow angle can be obtained only by adapting the radial location of the N 2D blade sections.

The extension to a full 3D method and application to the design of radial compressor impellers is described in [6] and [7].

3. Inverse design method

The outcome of the previous design system is a blade shape which is optimum with respect to the specified Objective Function. The only way the designer can influence the result is by modifying the penalties and their weights. The method itself finds out how the corresponding "optimum" Mach number distribution should look like. This important advantage however is at the cost of a large number of flow analyses on different geometries.

A more direct interaction with the flow, with less calculation effort, is possible by means of inverse methods defining the geometry corresponding to a desired velocity or pressure distribution along the blade contour. They allow a very detailed and local interaction with the flow. Such methods however are useful only if one has a clear idea of how an "optimum" pressure distribution looks like. This is rather well known for 2D flows [8] but needs further study for 3D flows when secondary flow phenomena become more important.

The main disadvantage of inverse design methods however is the difficulty to guarantee that the mechanical, geometrical and other constraints will be respected. This was especially difficult with traditional inverse methods, performing the calculations in an unphysical plane (hodograph method [9] and conformal mapping) because the designer could verify the constraint only after the solution has been mapped into the physical plane. This has been at the origin of a lot of disappointments and created a lot of reluctance to use inverse design methods. Today there is a better understanding of the relation between flow and geometry and some techniques have been developed to help the designer in this respect [10].

CFD methods solve the flow equations in the numerical domain with prescribed boundary conditions on the borders. These borders being the solution of the problem, all inverse design methods using CFD need to be iterative. They rarely start from scratch but are used mainly to improve the pressure or Mach number distribution along an existing blade profile.

Optimisation methods can be transformed into inverse design methods by specifying as penalty the difference between the present and a prescribed velocity distribution. Other inverse design methods calculate the impact of local geometry changes on the velocity distribution and use these sensitivities to define a geometry modification that will provide at each iteration a pressure distribution which is closer to the target. Both methods use pure numerical techniques to define the required geometry changes and need a lot of iterations before the target is reached.

The following method uses the flow equations to define the geometry modifications required to achieve the prescribed distribution. It has shown to converge

rapidly to the required geometry and is applicable to a large variety of design problems [11, 12]. The core of this design method is a time marching solution of the three-dimensional Euler equations in a domain of which the walls, that are the solution of the problem, are moving during the transient part of the calculation.

Two flow calculations are made at each time step (Figure 13).

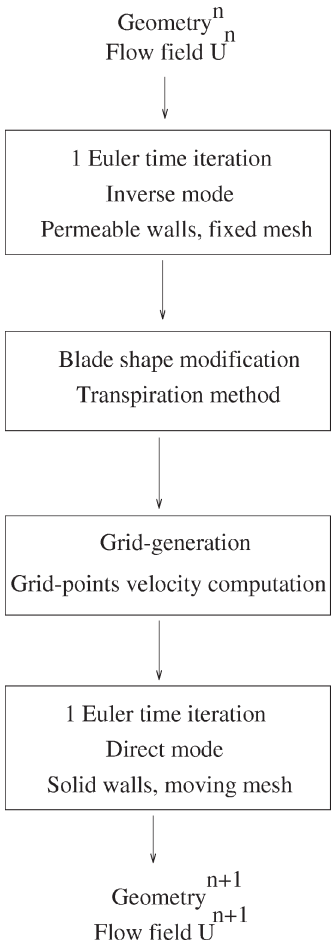

Figure 13. Flow chart of moving wall inverse design method

The first time step defines the flow corresponding to the required pressure distribution imposed on the blade walls of the present geometry. Except when the imposed pressure distribution equals the one resulting from a direct calculation around the same geometry, the calculated velocity will not be tangent to the walls. Using permeable wall boundary conditions one can calculate the velocity component normal to the blade walls which is then used to define a new blade geometry by means of the transpiration model (Figure 14). The magnitude of the displacement perpendicular to the existing blade surface (ξ^k_{out}) is obtained by applying the continuity in the cells between the old and new blade walls in function of the calculated normal and imposed tangential velocity along the initial blade suction and pressure side.

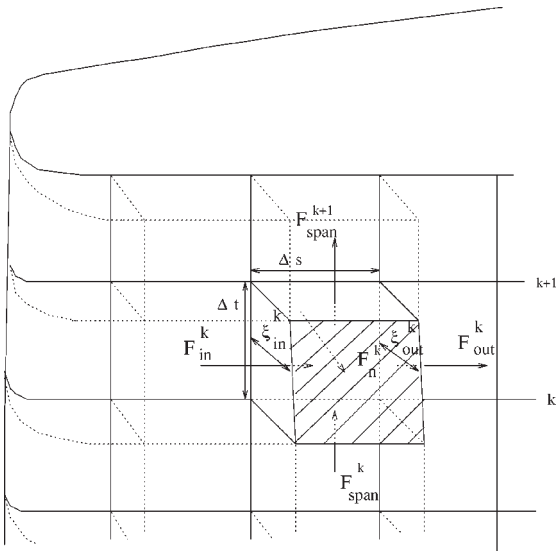

Figure 14. 3D transpiration method

The method progresses separately along both sides of the blades, from the stagnation line to the trailing edge. One can keep the stagnation line unchanged or modify it to achieve any required lean or sweep.

A new mesh is generated around the new profile after each blade shape modification. The displacements of all mesh points over the time step define the 'grid-point velocity' W_g.

The second time step makes an update of the flow field, taking into account the movement of the walls and mesh. Experience shows that after each time step the pressure distribution on the new geometry is closer to the target one, provided that this target corresponds to a realistic geometry. The direct Euler solver with moving walls is different from an Euler solver with fixed walls by the modified boundary conditions and the extra terms W_g related to the variation of the cell volume.

These two time steps are alternated in an iterative procedure until the normal velocity and hence the transpiration flux is zero, *i.e.* when the pressure distribution obtained during the analysis step equals the required one. In this procedure the geometry converges to the desired one simultaneously with the flow converging to the steady asymptotic solution. An on-line visualisation of the evolution of the blade geometry during the design process allows for an eventual adjustment of the target pressure distribution if the mechanical or other requirements are violated.

3.1. Existence and mechanical constraints

Before presenting some examples of inverse design it is of interest to pay attention to the question of existence of the solution. This question results form the complex relation between geometry and velocity or pressure and is closely related to the problem of mechanical constraints. Many theoretical studies have attempted to give an answer to it but the problem is still not solved. The three conditions for the velocity distribution, derived by Lighthill [13] for isolated wing sections, are necessary but not always satisfactory and of little use for practical designs with CFD.

The following conditions for blade cascades, illustrated in Figure 15, are equivalent to the three conditions of Lighthill. They can easily be verified before the design is started or being used to predict the effect of a velocity change on the blade thickness.

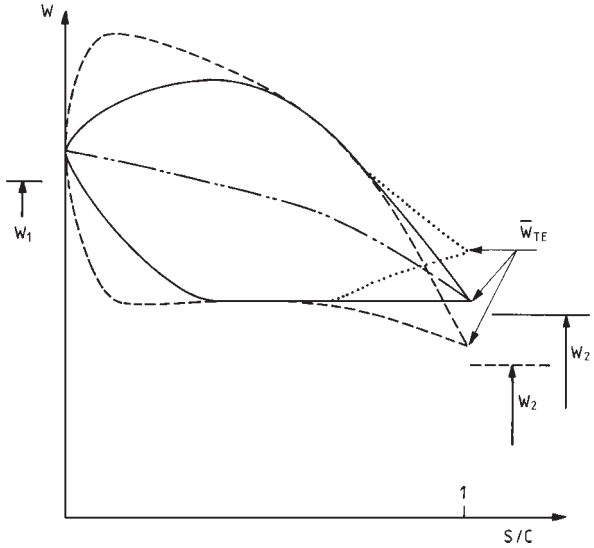

Figure 15. Variation of circulation and trailing edge velocity

- When a flow is approaching a blade, a difference between the suction and pressure side due to loading and an increase of the average velocity due to the leading edge thickness takes place. It is therefore necessary that the average of the velocities, imposed on pressure and suction side, is higher than the inlet velocity to allow for a positive blade thickness. This condition is equivalent to the first condition of Lighthill relating the blade velocity to the free stream velocity and can already be verified before starting the design.
- The second condition is obtained by requiring positive thickness of the trailing edge. The average trailing edge velocity must be higher than the outlet velocity. For incompressible irrotational flow the outlet velocity is known in advance from the following relations:

  Continuity:

$$W_{2x} = W_{1x} \tag{1}$$

  Irrotationality:

$$\oint W_{tg}.ds = W_x(\mathrm{tg}\,\beta_2 - \mathrm{tg}\,\beta_1)\, pitch \tag{2}$$

  This condition is equivalent to the second condition of Lighthill imposing that the suction and pressure side must join at the trailing edge (measured perpendicular to the flow) and can also be verified before starting to design. This condition is closely related to the next one because the modulus of the outlet velocity depends on the turning.
- Specifying the velocity along the suction and pressure contour does not guarantee that the blade lengths will join at the trailing edge (streamwise direction).

One can not define a priori how long the suction and pressure side must be to have a closed trailing edge. One may need to change the length of one side during the design process. This results in a change of circulation and hence a different outlet angle and velocity, unless also the pitch to chord ratio is adjusted.

Previous considerations are also very useful to satisfy the mechanical constraints. An increase of the average trailing edge velocity (—— to ·····) will result in an increase of the local blade thickness and a decrease of average velocity results in a reduction of blade thickness. Any change in blade loading changes the outlet flow angle and the average trailing edge velocity must be adjusted if one wants to keep the trailing edge thickness unchanged. More turning in compressors at constant mass flow (—— to − −) requires a decrease of the average trailing edge velocity if one wants to keep the trailing edge thickness constant. More turning in turbines at constant mass flow requires an increase of the average trailing edge velocity if one wants to keep the trailing edge thickness constant.

However an extra degree of freedom results from a modifications of the meridional contour and lean. It has an impact on the average velocity and allows satisfying mechanical constraints without changing the target velocity distribution [14, 15].

3.2. Uniqueness

The uniqueness of a solution is observed if, in addition to the pressure distribution on the suction and pressure side, also correct boundary conditions are imposed at the inlet and outlet. The relation between the axial velocity (mass flow) and outlet flow angle is given by Equation (2).

Different combinations of W_x and $\mathrm{tg}\beta_2$ are possible for a given β_1 and given integral of the velocity distribution. Prescribing the outlet static pressure, as in the analysis problem, is no longer a sufficient condition to obtain a unique solution because the mass flow depends on the blade trailing edge shape which is to be defined. At a prescribed trailing edge velocity, every trailing edge angle corresponds to a different blade trailing edge thickness. In the Navier-Stokes version of the design program, this has an impact on losses. Hence the outlet static pressure is influenced by the outlet flow angle. Keeping the outlet static pressure constant will result in a change of mass flow.

Convergence to a unique solution is sometimes hard to achieve when keeping the outlet static pressure constant. This is particularly difficult in turbines with high turning because the mass flow and outlet flow angle are continuously changing when using the inverse Navier-Stokes method. The blade shapes shown in Figure 16 are solutions of a design with the same surface pressure distribution, inlet total pressure and temperature. Table 2 lists the corresponding outlet flow conditions. They are obtained at different instants during the design process. The change in losses with trailing edge thickness explains the small differences in outlet Mach number at constant outlet pressure in Table 2. The table also shows a variation in mass flow that is in agreement with the change in flow angle at a given outlet Mach number. One can conclude that a unique solution is possible if in addition to P_o, T_o and β_1 one also imposes the constant mass flow instead of the outlet static pressure. This is however not a straightforward matter in Euler and Navier-Stokes solvers.

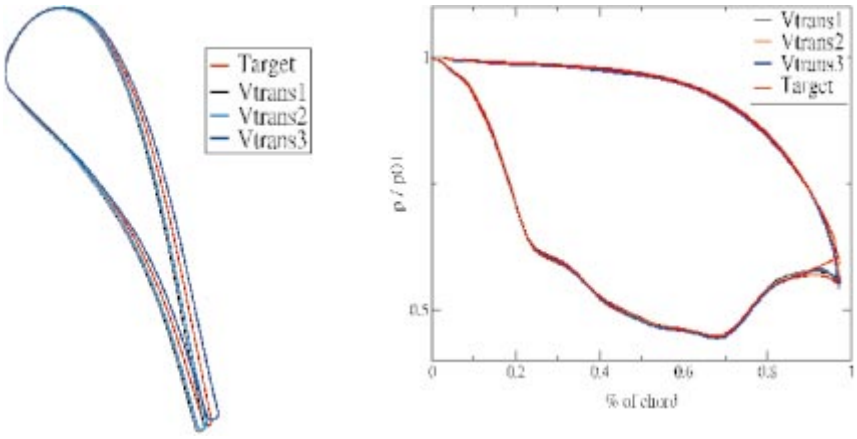

Figure 16. Different blade shapes providing the same pressure distribution

Table 2. Cascade outlet flow conditions

	original	Vtrans1	Vtrans2	Vtrans3
β_2	-74.6°	-75.4°	-75.2°	-73.9°
M_2	0.937	0.950	0.954	0.940
Mis_2	0.970	0.987	0.992	0.976
Δm		-5.5%	-4.4%	$+3.3\%$

Previous relations between the velocity and geometry are relatively simple for axial turbomachinery with irrotational flows but become particularly complex for radial impellers where the flow is rotational depending as well on geometry as on the rotational speed. Special techniques such as hybrid design systems and design with a parameterised target have been developed to facilitate the control of the mechanical constraints. Both methods are illustrated by following designs.

3.3. Redesign of a transonic compressor blade with a hybrid method

The hybrid version of the inverse design method is illustrated by the redesign of a transonic compressor rotor with 14 highly twisted blades rotating at 31264 RPM. The hub/tip diameter ratio is 0.5 at the inlet, and the meridional view shows a non-negligible contraction of the passage (Figure 17).

The flow field around the initial geometry has been calculated for an outlet isentropic Mach number of 0.76 at the mean radius. Non periodic H-grids are used to discretise the numerical domain. The inlet relative Mach number varies from 0.74 at the hub section, to 1.35 at the tip. The calculated isentropic Mach number distribution on the blade tip section is shown by + in Figure 18.

The inverse design method has been used to redesign the blade, prescribing a shock free Mach number distribution at five equidistant sections between hub and shroud. The required tip section Mach number distribution is indicated by $\diamond$ in Figure 18. Imposing the Mach number distribution on both the suction and pressure side does not allow the control of the blade thickness. Imposing the new Mach number distribution on the suction side and keeping the pressure side Mach number

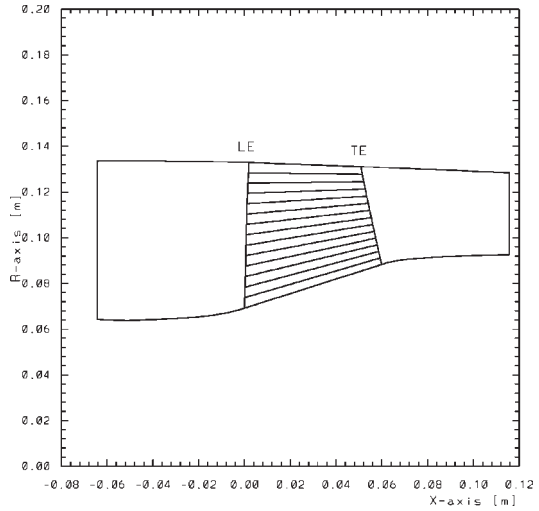

Figure 17. Meridional view

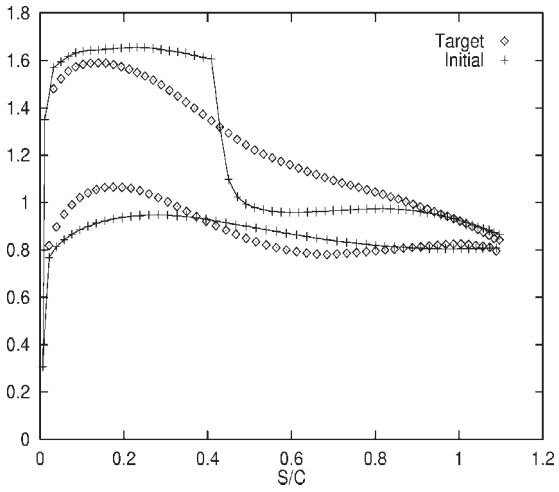

Figure 18. Initial (+) and imposed (◇) isentropic Mach number distributions – tip section

unchanged, results in a very thin blade in the first half and a too thick blade in the second half of the chord. One has therefore an advantage in using a hybrid version of the method in which the suction side Mach number and the blade thickness are imposed.

The pressure distribution is not prescribed on the blade pressure side but recalculated at each analysis step [10, 11]. Each time the suction side geometry is redefined by the transpiration method, the pressure side is adapted to keep the blade thickness distribution unchanged. In this way the method itself predicts the pressure side Mach number distribution that is compatible with the constraint on the blade thickness.

The new pressure side Mach number distribution shows more diffusion than the initial one, and is therefore less optimum from the aerodynamic point of view (Figure 18). However satisfying the thickness constraint by adjusting the suction side

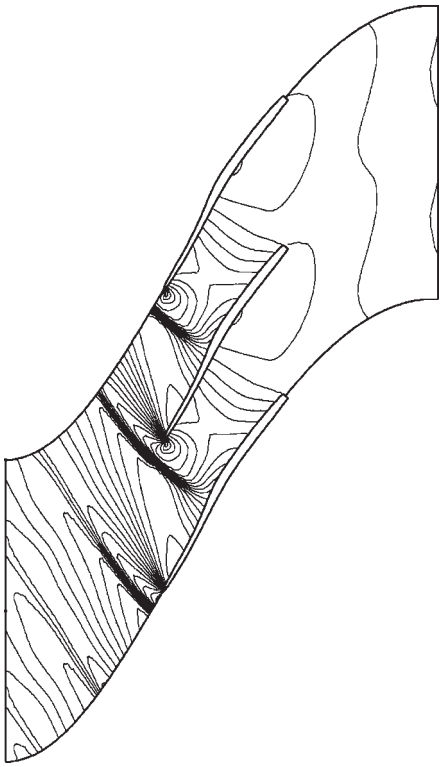

Figure 19. Iso-density lines – final blade – tip section

Mach number distribution would have resulted in a less efficient blade. The iso-density lines at the redesigned shroud section are shown in Figure 19. The figure illustrates how the S shaped suction side generates compression waves that converge into a bow shock, which does no longer interact with the suction side boundary layer.

The initial and final blade geometries at hub, mean and tip are compared in Figure 20. One observes that the blade thickness distribution is conserved at each cross section.

Euler solvers do not account for viscous effects, and the suction and pressure side boundary layer displacement thickness is included in the designed blade. This is not a big problem because the boundary layer displacement thickness can already be calculated from the prescribed Mach number distribution, even before the blade geometry is known. The sum of the geometrical thickness and boundary layer displacement thickness at the trailing edge is imposed as a constraint on the designed geometry. After completing the inverse design of the blade, the boundary layer displacement thickness is subtracted, to obtain the "metal" blade shape as shown in Figure 21.

3.4. Design of turbine blade with a parameterised target

A clear relation between the blade loading (circulation) and outlet flow angle exists only for 2D potential flows. In 3D flows the requirement to obtain a prescribed value of the outlet flow angle is more easily satisfied by introducing the possibility to adjust the velocity distribution and hence the circulation during the design procedure.

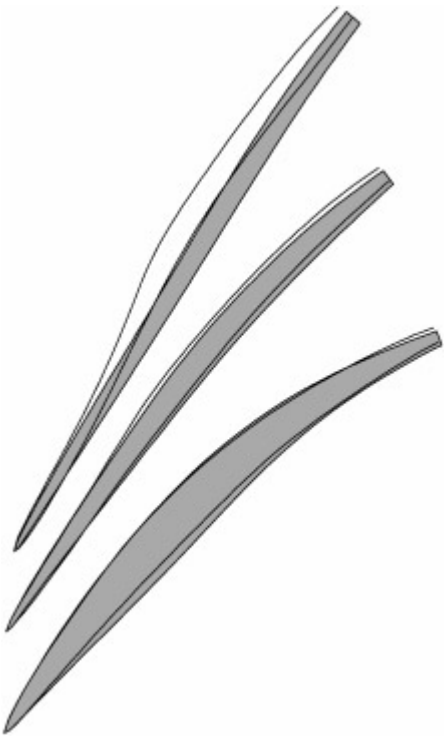

Figure 20. Initial (grey) and final geometries: hub, mean and tip sections

Figure 21. Subtraction of the boundary layer: mean section

The outlet flow angle and blade trailing edge thickness being closely related to each other, this procedure can be used to adjust the blade trailing edge thickness to the pre-set value.

A possible way of handling this problem is by imposing a parameterised suction or pressure side Mach number distribution and to adjust the parameters during the design until the required outlet angle and the trailing edge thickness are obtained. This feature is illustrated by redesigning the blade section of a turbine annular cascade to correct for the unfavourable effect of a 30° compound lean (Figure 22) on the suction side velocity distribution. The increase of loading at mid-span resulted in a bump in the suction side velocity distribution (Figure 23). Three different target Mach number distributions have been defined. They are functions of a parameter, between 0 and 1, which is varied during the design process until the pre-set outlet flow angle is obtained. Full convergence inclusive adjustment of β_2 within less than 0.2° is obtained after 4 000 time steps.

3.5. Extension to viscous inverse design

The inverse procedure presented here has originally been developed in combination with an Euler solver. The extension to viscous flow is not straightforward because the no-slip condition (zero velocity on the walls) is not compatible with the permeable wall concept and complicates the reconstruction of the blades by the transpiration technique. First results, obtained with a Navier-Stokes solver, are described in [16]

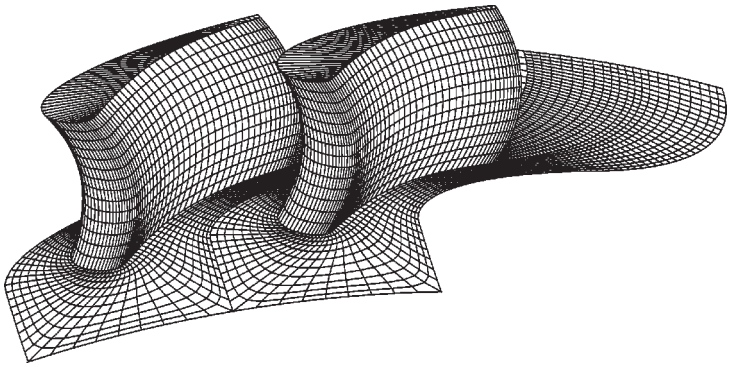

Figure 22. Turbine stator with 30° compound lean

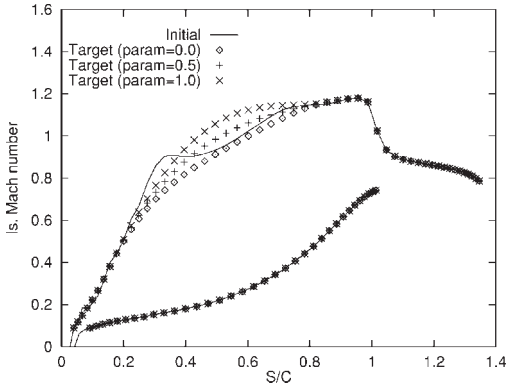

Figure 23. Parameterised target on the suction side

and [17]. They use an approximate definition of the transpiration velocity and are not very robust. More recently a new approach has been developed by de Vito [18]. He combines the viscous flow calculation around the blade, by means of a Navier-Stokes solver (the analysis phase), with an Euler solver on a restricted mesh close to the blade, for the design phase. The method has shown to take more time than an inverse Euler solver but the final blade shape does not need to be corrected anymore for viscous blockages and the method is very robust. Figure 24 shows the initial and final blade shape and Mach number distribution. Figure 25 shows the result of the redesigned transonic turbine blade. The smooth suction side Mach number distribution is the consequence of an expansion at the location where the trailing edge shock impinges on the suction side.

4. Conclusions

The modern methods, of which two have been presented in this paper, are efficient tools for the design of turbomachinery blades by shortening the lead time and providing high performance.

Approximate model design systems, based on an Artificial Neural Network and Genetic Algorithm allow a considerable speed-up of the optimisation techniques. These self-learning systems make full use of the expertise gained during previous designs. They can be used with any flow solver and do not require the definition

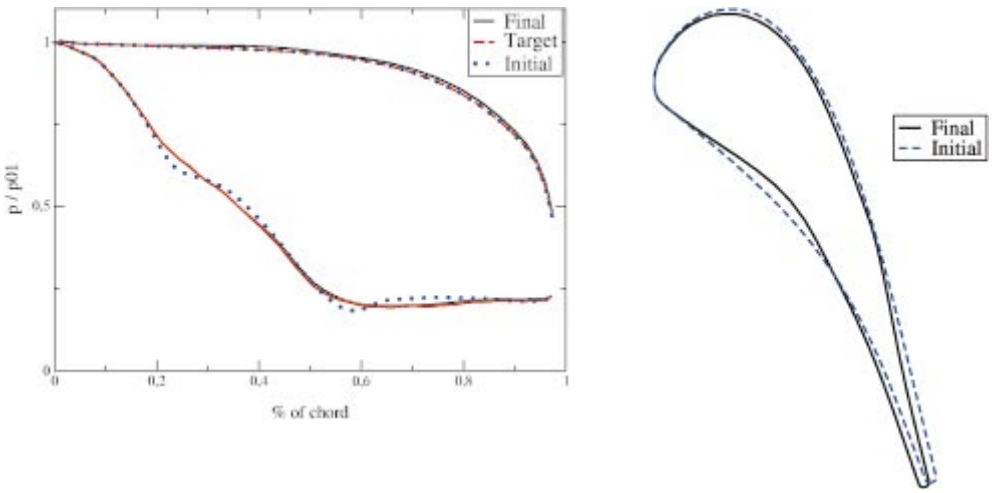

Figure 24. Mach number distribution and shape of the original blade and target blade

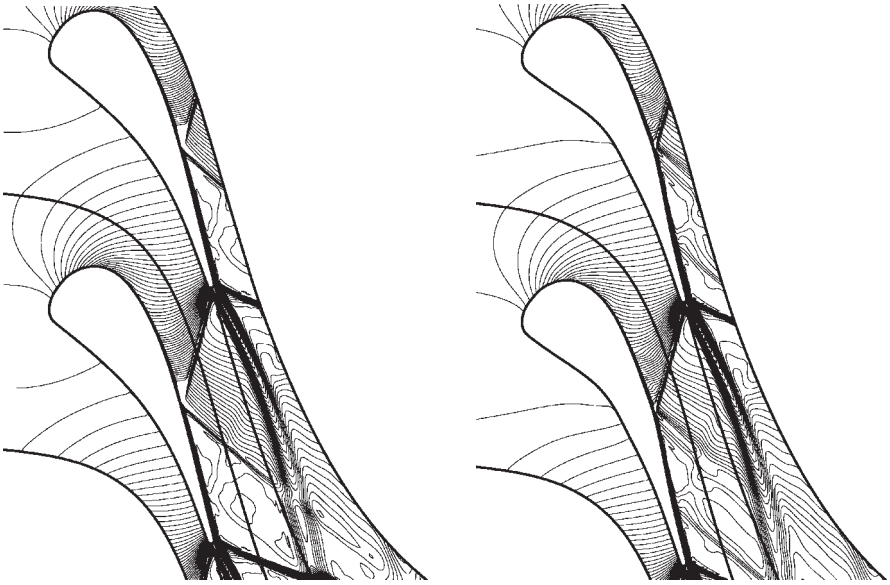

Figure 25. Iso-Mach lines in the original and redesigned blade passage

of a target pressure or Mach number distribution. The outcome of such a global optimisation depends on the accuracy by which the design target and constraints are expressed in the Objective Function.

Inverse methods allow a much more detailed and local control of the flow by means of the target pressure distribution. Optimising the target is rather easy for 2D flows but much more difficult for 3D geometries where secondary flows have an important impact on losses. The method requires a modification of the boundary conditions of the flow solver and it is more difficult to account for mechanical constraints. However, the hybrid version of the method and the use of parameterised targets are powerful extensions of the basic method.

References

[1] Thilmany J 2000 *Mechanical Engineering* **11** 98

[2] Pierret S and Van den Braembussche R A 1999 *ASME J. Turbomachinery* **121** 326

[3] Vanderplaats G N 1984 *Numerical Optimization Techniques for Engineering Design*, McGraw-Hill

[4] Pierret S, Demeulenaere A, Gouverneur B, Hirsch Ch and Van den Braembussche R A 2000 *AIAA Paper* **2000-2479**

[5] Pierret S and Van den Braembussche R A 1998 *Proc. RTA/AVT Symposium on Design Principles and Methods for Aircraft Gas Turbine Engines*, Toulouse, RTO-MP-8

[6] Cosentino R, Alsalihi Z and Van den Braembussche R A 2001 *Proc. 4th European Conference on Turbomachinery*, Florence, Italy, pp. 481–490

[7] Rini P, Alsalihi Z and Van den Braembussche R A 2001 *Proc. 5th ISAIF*, Gdansk, Poland, pp. 535–547

[8] Papailiou K D 1971 *ASME J. Eng. for Power* **93** 147

[9] Sanger N L and Schreeve R P 1986 *ASME J. Turbomachinery* **108** 43

[10] Demeulenaere A and Van den Braembussche R A 1998 *Proc. RTA/AVT Symp. Design Principles and Methods for Aircraft Gas Turbine Engines*, Toulouse, France, RTO-MP-8

[11] Demeulenaere A and Van den Braembussche R A 1998 *ASME J. Turbomachinery* **120** 247

[12] Demeulenaere A and Van den Braembussche R A 1999 *J. Inverse Problems in Engineering* **7** (3) 235

[13] Lighthill J M 1945 *A new method of two dimensional aerodynamic design* ARC R&M 2112

[14] Demeulenaere A, Leonard O and Van den Braembussche R A 1998 *ASME Paper* **98-GT-127**

[15] Passrucker H and Van den Braembussche R 2000 *ASME Paper* **2000-GT-457**

[16] Demeulenaere A, Leonard O and Van den Braembussche R A 1997 *Proc. 2nd European Turbomachinery Conference on Turbomachinery, Fluid Dynamics and Thermodynamics*, Antwerpen, Belgium, pp. 339–346

[17] Wang Z, Cai R, Chen H and Zhang D 1998 *ASME Paper* **98-GT-126**

[18] de Vito L and Van den Braembussche R A 2001 *A Novel Viscous Inverse Design Method: Blending a Navier-Stokes Solver for the Analysis with an Euler Solver for the Inverse Design* VKI Pr-2001